ISSN: 2472-3703 DOI: 10.6911/WSRJ.202507_11(7).0001

Optimized Design of the Grasping Mechanism for Floating Island Vegetation Laying Boat

Kambale Mughanda[1], Haipeng Yan[2,*], Xiongfei Yan[2], Zhenduo Yang[3], Changyu Wang[4], Zhuo Chen[3] and Jia Zhang[3]

[1]School of International Education, Hebei University of Science and Technology, Shijiazhuang, China

[2]School of Mechanical Engineering, Hebei University of Science and Technology, Shijiazhuang, China

[3]College of environmental science and engineering, Hebei University of Science and Technology, Shijiazhuang, China

[4]FedUni Information Engineering Institute, Hebei University of Science and Technology, Shijiazhuang, China

[*]Corresponding author: lnyanhp@126.com

Abstract

To address the technical challenges of accurate deployment of ecological floating islands in dynamic water environments, this study proposes an intelligent operation system integrating high-precision positioning and adaptive grasping capabilities. Through hydrodynamic disturbance spectrum analysis, a wave-structure coupling dynamic model was established, and an innovative composite control strategy based on PID control and wave feedforward compensation was developed. At the same time, the system adopts a three-degree-of-freedom spatial motion structure, integrating a non-contact electromagnetic adsorption end effector with a funnel guidance structure, achieving adaptive grasping within a load range of 10±2 kg, and completely avoiding damage to the HDPE surface. By optimizing the design of the clamping mechanism, its static stiffness was increased by 42%, and the fatigue life exceeded 1×10^6 cycles. This design effectively solves the precise operation challenges of floating island engineering equipment in dynamic water environments, providing key technical support for the large-scale application of ecological floating island technology.

Keywords

Ecological Floating Island; Dynamic Water Disturbance; Adaptive Grasping; Electromagnetic Adsorption Technology; Positioning Accuracy.

1. INTRODUCTION

At present, ecological floating island technology has become a major solution for the treatment of eutrophicated waters. However, its large-scale application is limited by issues such as low operational efficiency, high maintenance costs, and significant safety risks. The root cause lies in the lack of intelligent operational equipment, especially in the field of precise adaptive grasping technology for floating island vegetation, where there are certain deficiencies. Deviations in grasping positions and insufficient grasping positioning accuracy can lead to mechanical interference between the floating island frame and the boat body, thereby damaging the HDPE floating island buckle structure and causing the composite fiber floating island fixing

ISSN: 2472-3703 DOI: 10.6911/WSRJ.202507_11(7).0001

system to fail. Moreover, under wind and wave conditions, it is prone to impact overload (dynamic load reaches 2-3 times the static load), leading to the destruction of the vegetation module structure. Therefore, the development of a multi-functional floating island vegetation deployment and inspection boat (deployment and inspection boat) integrating high-precision intelligent positioning grasping technology has become a key breakthrough direction to promote the large-scale application of this technology.

The research direction of adaptive grasping technology is mainly divided into three categories: rigid underactuated grasping mechanisms [1], soft grasping mechanisms [2-4], and compliant grasping mechanisms [5-12]. The rigid underactuated grasping mechanism has a number of actuation units less than the number of degrees of freedom, which can passively adapt to the shape of the grasping object by utilizing the unactuated degrees of freedom that are not controlled by the actuation [13-14]. However, the rigid underactuated grasping mechanism has a rigid contact relationship with the grasping object, and it can directly transmit the rigid impact of the actuation units, which can easily damage fragile and deformable operational objects. Soft grasping mechanisms have good shape adaptability, but they generally use pneumatic or dielectric elastomers with lower motion resolution and slower response speeds for actuation [15], making it difficult to accurately and in real-time control the pose and load. Compliant mechanisms use material elastic deformation to achieve the transmission or conversion of force or motion, and have the advantages of integrated molding and no assembly, which have been widely used in fields such as micro and nano operations that require high precision in motion. However, the viscoelastic characteristics of flexible materials lead to slow response speeds of the grasping mechanism. At the same time, the low elastic modulus characteristics of flexible materials lead to low out-of-plane stiffness of the mechanism, affecting the load-bearing capacity.

To address the current issue of insufficient adaptability of floating island deployment equipment in dynamic water environments, this study, based on hydrodynamic disturbance spectrum analysis (wave frequency 0.1-1.2 Hz, amplitude ±0.5 m), innovatively proposes a high-precision adaptive grasping mechanism with real-time pose compensation, filling the technological gap in precise deployment equipment for floating islands in dynamic waters.

2. SGRASPING MECHANISM DESIGN

This grasping and laying mechanism takes the lifting device as its core, integrating electromagnetic adsorption technology with a funnel-type guidance structure to achieve high-precision positioning of the floating island modules. Compared to traditional lifting devices, this device dynamically adjusts the joint torque (τ) based on a PID control algorithm, effectively suppressing the vibration amplitude of the end effector, thereby ensuring the morphological integrity of the plant root system during transplantation. At the same time, its end effector uses a non-contact electromagnetic adsorption technique, avoiding mechanical contact with the floating island surface, that is, the high-density polyethylene (HDPE) surface coating, meeting the interface requirements for the uniform growth of biological films.

2.1. Transfer mechanism design

As shown in Figure 1, the main body of the mechanism is a three-degree-of-freedom (3-DOF) spatial motion system. The driving torque of its core rotary joint can be adaptively adjusted based on the real-time changes in dynamic load conditions, enhancing the pose stability of the end effector by suppressing multi-body coupled vibrations in real time. This control strategy has become the core technology to ensure the spatial positioning accuracy and consistency of contact force during the laying process of the vegetation module, effectively solving the dynamic instability issues during the flexible transplantation of the floating island modules.

ISSN: 2472-3703 DOI: 10.6911/WSRJ.202507_11(7).0001

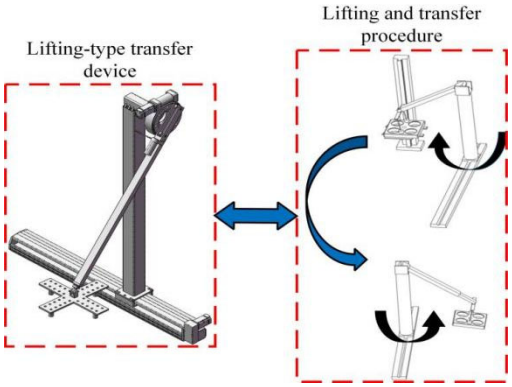

Figure 1. 3-DOF boom mechanism and motion sequence diagram

The operation condition analysis of the deployment and inspection boat indicates that the floating angle θ of the crane mechanism must satisfy θ≥±60° to cover the working space. Based on this process constraint, the load torque model (τ) established is shown in Equation (1), which comprehensively considers the fluid resistance torque (including the wave disturbance term), inertial coupling effects, and the nonlinear characteristics of joint friction.

$$\tau = G \bullet L sin\theta \tag{1}$$

In the equation, g represents the acceleration due to gravity (taken as 9.8m/s2); m is the mass of the object; G is the load; and L is the maximum outreach distance.

This model is embedded into a PID closed-loop control framework, where the control output is dynamically adjusted in real-time through parameter identification to achieve dynamic compensation of the crane driving motor speed

2.2. Optimization of end-effector gripping mechanism

The end effector of this mechanism utilizes a non-contact electromagnetic adsorption technology, coupled with a funnel-type guidance structure, as shown in Figure 2. This composite design significantly enhances the grasping fault tolerance of the floating island modules.

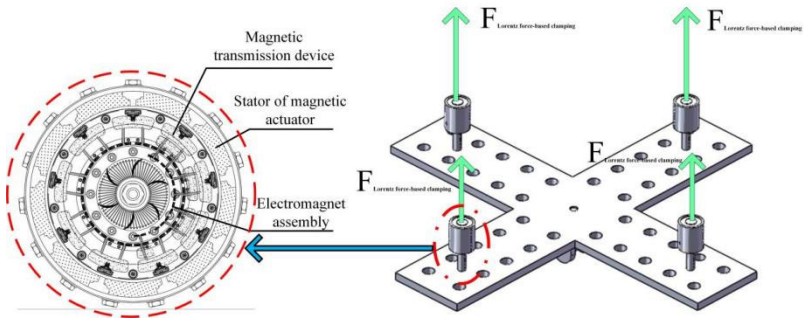

Figure 2. Magnetic end-effector gripping mechanism and schematic diagram

According to the parameters of the floating island vegetation module shown in Table 1, the target grasping mass is approximately 10 kg, but there is a dynamic mass fluctuation of 50% in actual operations. In addition, the ultimate tensile strength limit of the embedded metal plates in the modules (304 stainless steel, thickness 1.2 mm) imposes strict constraints on the adsorption force.

ISSN: 2472-3703 DOI: 10.6911/WSRJ.202507_11(7).0001

Table 1. Floating island vegetation layout parameters

Type	Size	floating island thickness	root and rhizome penetration depth
plastic ecological floating island	2000×1500×170mm	5-10 cm	≤30 cm
composite fiber	2000×1500×170mm	8-16 cm	≤1.5 m

To address this, a dynamic model of electromagnetic adsorption force as shown in Equation (2) was established. Combined with a variable gain PID control algorithm, it calculates in real-time: the mass-inertia coupling term, as well as the safety threshold of metal sheet stress. Thereby, it dynamically suppresses impact loads, ensuring that the stress on the metal sheet remains within the elastic deformation region at all times.

$$F_{Electromagnetic\ adhesion} = mg \bullet S \tag{2}$$

In this context, g represents the acceleration due to gravity (9.8 m/s^2); m denotes the mass of the object; S is the safety factor (with a value of 1.5).

3. DESIGN OF STACKING MECHANISM BASED ON WATER WAVE DISTURBANCE

The operating environment for the multi-functional floating island deployment and inspection boat is an open water area. The natural water environment has certain minor waves, and the continuous excitation of these disturbances can lead to multi-degree-of-freedom coupled oscillations between the floating island modules and the laying platform. To address this, on the basis of the aforementioned grasping mechanism, an innovative stacking clamping device has been proposed, as shown in Figure 3. This device uses a bidirectional hydraulic synchronous locking mechanism, combined with an adaptive rubber cushion, which can effectively improve the grasping and laying accuracy of the floating island vegetation mechanism in this disturbed water environment.

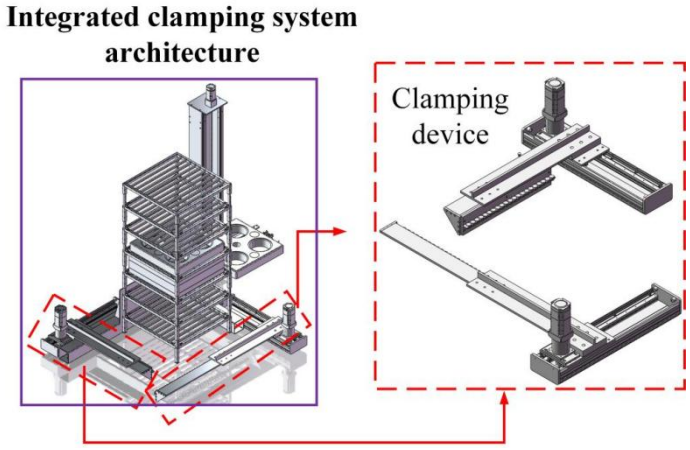

Figure 3. Stacking device architecture

3.1. Analysis of Grasping Deviation Based on Water Wave Disturbance

Based on shallow water wave theory, a small-amplitude linear wave dynamic model as shown in Equation (3) is established. This model uses Fast Fourier Transform (FFT) to solve the wave surface elevation in real time, thereby constructing a displacement deviation model,

ISSN: 2472-3703 DOI: 10.6911/WSRJ.202507_11(7).0001

which provides a feedforward compensation model for the subsequent design of the stacking mechanism.

$$\frac{\partial^2 u}{\partial t^2} = C^2 \left(\frac{\partial^2 u}{\partial x^2} + \frac{\partial^2 u}{\partial y^2} \right) \tag{3}$$

In the equation, u(x,y,t) represents the disturbance in water surface elevation; c is the wave speed (under shallow water conditions, $c=gh$, where g is the acceleration due to gravity and h is the water depth).

Since the disturbances from the water surface are primarily manifested as heave displacement, pitch angle, and roll angle, and these dynamic interferences are nonlinearly coupled with the water surface elevation disturbance function $u(x,y,t)$. Therefore, based on the water surface disturbance model and combining frequency domain response analysis, the vertical displacement transfer function $\Delta z(t)$ is obtained, as shown in Equation (4). This provides a theoretical basis and technical support for the wave compensation control of floating island engineering equipment.

$$\Delta z(t) = u(x_0,\ y_0,\ t) \tag{4}$$

Under the excitation of waves, the floating island system will exhibit significant asymmetric fluid dynamic responses. That is, when one side of the floating island at the wave crest phase is lifted by the positive wave pressure F, the side at the wave trough phase experiences a negative buoyancy difference. The resulting torque difference causes the floating island to develop dynamic attitude angles θ(t). Based on rigid body kinematics analysis, an instantaneous position offset model as shown in Equation (5) is established.

$$\Delta x = L \bullet tan(\theta(t)) \approx L \bullet \theta(t) \tag{5}$$

3.2. Optimized design of the clamping mechanism

The clamping mechanism, as shown in Figure 4, employs a dual-drive collaborative gripping system. Through the synergistic effect of modular servo drive units and multi-modal gripping strategies, it achieves precise constraint of the floating island modules with multiple degrees of freedom.

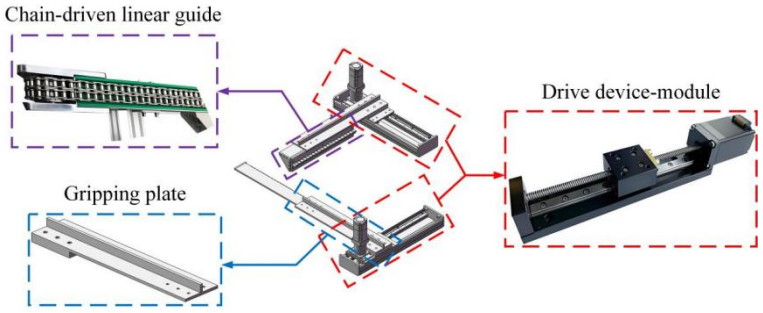

Figure 4. Floating island clamping plate architecture

3.2.1 Simulation analysis of key components of the clamping mechanism

The connecting plate, as the core functional component of the clamping device, is responsible for the precise positioning and rigid clamping of the floating island modules in the three-

ISSN: 2472-3703 DOI: 10.6911/WSRJ.202507_11(7).0001

dimensional storage system. The structural performance directly determines the pose repeat accuracy of subsequent stacking operations. To ensure that this key component meets the operational requirements of this working condition, structural static mechanical simulation analysis and optimization design are carried out based on the finite element simulation platform. The specific process is as follows:

(1) Material parameter definition: The connecting plate is made of Q235 low-carbon steel, and its key mechanical performance parameters are shown in Table 2, including the modulus of elasticity (E), Poisson's ratio (v), yield strength (σ_s), and density (ρ);

Table 2. Material parameters of the model

Material	modulus of elasticity/ (Mpa)	Poisson's ratio	density/ (kg/mm3)
ZG230-450	2.07e5	0.28	7.85e-6

(2) Meshing: By comparing the convergence analysis of methods such as free meshing, mapped meshing, and adaptive meshing, the free meshing scheme was ultimately adopted. This method, based on the Delaunay triangulation algorithm, automatically generates second-order tetrahedral elements and implements local refinement in areas of stress concentration. The meshing result is shown in Figure 5;

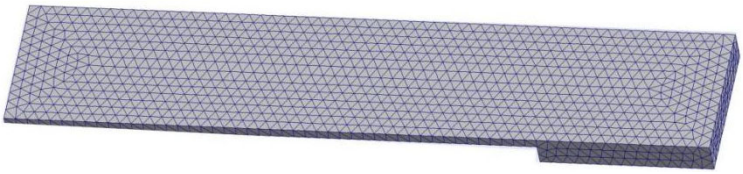

Figure 5. Mesh generation results

(3) Definition of boundary conditions:

① Based on a single-degree-of-freedom system architecture, establish contact pairs (i.e., where the connecting plate is connected to the gear rack mechanism);

② Apply fixed constraints at the connection between the connecting plate and the gear rack mechanism (i.e., the supporting part of the connection);

③ Considering the cantilever beam effect under load conditions, apply an equivalent concentrated load at the front end of the clamping plate, and add the corresponding load at this location;

The distribution results of the above boundary conditions are shown in Figures 6(a) and 6(b).

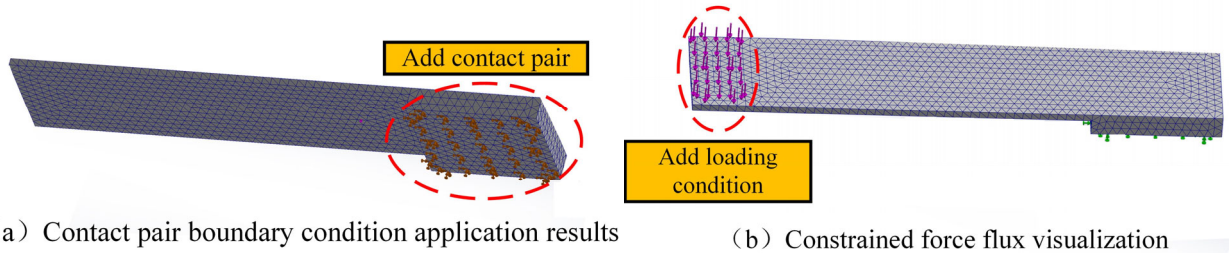

（a）Contact pair boundary condition application results （b）Constrained force flux visualization

Figure 6. Boundary condition application results in FEM analysis

(4) Results of static analysis: Finite element calculations indicate that the initially designed connecting plate exhibits significant structural defects under rated working conditions (Figure

ISSN: 2472-3703 DOI: 10.6911/WSRJ.202507_11(7).0001

8). The maximum deformation of 1.996 mm occurs at the cantilever end (exceeding the allowable value of 1.2 mm), and the stress concentration area (19.66 MPa) is located at the root of the gear engagement. The estimated fatigue life is only 2.3×10^4 cycles, which does not meet the requirements for continuous operation.

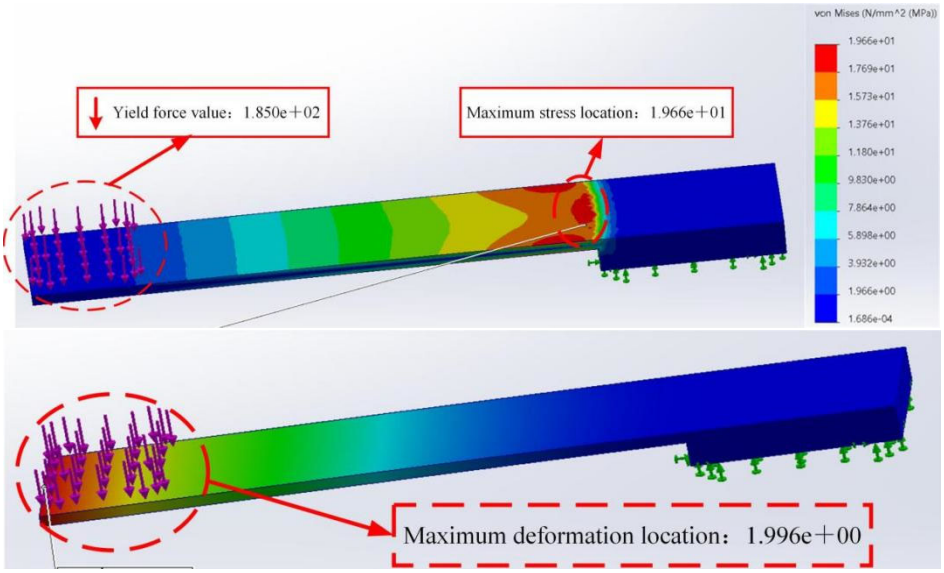

Figure 7. Boundary condition application results in FEM analysis

3.2.2 Optimization of the clamping plate

Based on the finite element analysis results, a topological optimization design was implemented for the connecting plate (Figure 8). By adding radial reinforcement ribs (with a thickness of 12 mm and a height of 25 mm) and optimizing the layout of the rib plates, the structural stiffness was increased by 42%. A verification simulation analysis was conducted on the optimized clamping plate mechanism (Figure 10), and the results showed that the maximum deformation of the structure was reduced to 0.82 mm (a reduction of 58.9%), the peak stress was decreased to 11.7 MPa (a decrease of 40.5%), and the first-order natural frequency was increased to 102 Hz (an improvement of 20%). As shown in Table 3, all key parameters meet the design requirements, verifying the effectiveness of the optimization plan and solving the problem of elastic deformation under clamping conditions.

Figure 8. Optimized clamping plate model

Table 3. Parameters related to the model optimized

Model	Total Deformation/ (mm)	Equivalent Stress/ (Mpa)	Quality/ (kg)
original model	1.996	19.66	13
optimized model	0.223	11.26	15

ISSN: 2472-3703 DOI: 10.6911/WSRJ.202507_11(7).0001

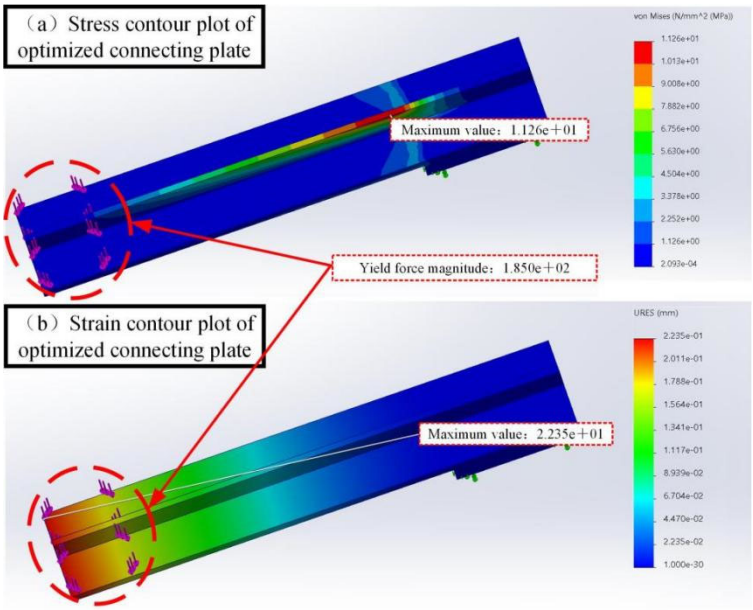

Figure 9. Finite Element Analysis Results of the Optimized Model

Static analysis indicates that the mass of the optimized connecting plate increased from 13 kg to 15 kg (an increase of 15.4%), but the key performance has been significantly improved: the maximum deformation was reduced from 1.996 mm to 0.223 mm (a reduction of 88.8%), and the maximum stress of 19.66 MPa is much lower than the yield strength of Q235 steel (σs = 235 MPa, safety factor n = 12). The optimization plan achieves a balance between stiffness enhancement and lightweighting, fully meeting the operational requirements.

4. CONCLUSIONS

To address the technical challenges of accurately deploying floating island vegetation in dynamic water environments, an innovative high-precision adaptive grasping system with real-time pose compensation capabilities has been developed. Through systematic research that includes theoretical analysis, numerical simulation, and structural optimization, a composite control strategy based on hydrodynamic disturbance spectrum analysis was proposed. This strategy integrates PID closed-loop control with wave feedforward compensation algorithms to improve the positioning accuracy of floating island modules and effectively suppress multi-degree-of-freedom coupled oscillations. Secondly, a non-contact electromagnetic adsorption end effector was designed and developed, in conjunction with a funnel guidance structure, to achieve adaptive grasping within the load range while completely avoiding damage to the HDPE surface. Lastly, the clamping mechanism was optimized, and simulation results showed that the static stiffness of the optimized mechanism increased by 42%, the first-order natural frequency reached 102 Hz, and the fatigue life exceeded 1×10^6 cycles. This design integrates high-precision intelligent positioning and grasping technology, effectively solving the precise operation challenges of floating island engineering equipment in dynamic water environments, and further promoting the large-scale application of ecological floating island technology.

ACKNOWLEDGEMENTS

The authors gratefully acknowledge the financial support from Research and Practice Project on Innovation and Entrepreneurship Education Teaching Reform in Higher Education Institutions in Hebei Province (2023cxcy088) and Collaborative Education Project of Industry University Research by the Ministry of Education (2410314936 and 2412030712).

ISSN: 2472-3703 DOI: 10.6911/WSRJ.202507_11(7).0001

REFERENCES

[1] Kobayashi A, Yamaguchi K, Kinugawa J, et al. Analysis of precision grip force for uGRIPP (underactuated gripper for power and precision grasp)[C]//2017 IEEE/RSJ International Conference on Intelligent Robots and Systems (IROS). IEEE, 2017: 1937-1942.

[2] Zhang H, Kumar A S, Fuh J Y H, et al. Design and development of a topology-optimized three-dimensional printed soft gripper[J]. Soft robotics, 2018, 5(5): 650-661.

[3] Brown E, Rodenberg N, Amend J, et al. Universal robotic gripper based on the jamming of granular material[J]. Proceedings of the National Academy of Sciences, 2010, 107(44): 18809-18814.

[4] Chen Y, Guo S, Li C, et al. Size recognition and adaptive grasping using an integration of actuating and sensing soft pneumatic gripper[J]. Robotics and Autonomous Systems, 2018, 104: 14-24.

[5] Krishnan S, Saggere L. Design and development of a novel micro-clasp gripper for micromanipulation of complex-shaped objects[J]. Sensors and Actuators A: Physical, 2012, 176: 110-123.

[6] Boudreault E, Gosselin C M. Design of sub-centimetre underactuated compliant grippers[C]//International Design Engineering Technical Conferences and Computers and Information in Engineering Conference. 2006, 42568: 119-127.

[7] Foody J, Maxwell K, Hao G, et al. Development of a low-cost underactuated and self-adaptive robotic hand[C]//International Design Engineering Technical Conferences and Computers and Information in Engineering Conference. American Society of Mechanical Engineers, 2014, 46377

[8] Huang M, Lu Q, Chen W, et al. Design, analysis, and testing of a novel compliant underactuated gripper[J]. Review of Scientific Instruments, 2019, 90(4).

[9] Petković D, Jovic S, Anicic O, et al. Analyzing of flexible gripper by computational intelligence approach[J]. Mechatronics, 2016, 40: 1-16.

[10] Petković D, D. Pavlović N, Shamshirband S, et al. Development of a new type of passively adaptive compliant gripper[J]. Industrial Robot: An International Journal, 2013, 40(6): 610-623.

[11] Liu C H, Chiu C H. Optimal design of a soft robotic gripper with high mechanical advantage for grasping irregular objects[C]//2017 IEEE International Conference on Robotics and Automation (ICRA). 2017: 2846-2851.

[12] Liu C H, Chen T L, Chiu C H, et al. Optimal design of a soft robotic gripper for grasping unknown objects[J]. Soft robotics, 2018, 5(4): 452-465.

[13] Cui J, Yan S, Hu J, et al. A metric to design spring stiffness of underactuated fingers for stable grasp[J]. Robotics and Autonomous Systems, 2018, 102: 1-12.

[14] Saliba M A, De Silva C W. Quasi-dynamic analysis, design optimization, and evaluation of a two-finger underactuated hand[J]. Mechatronics, 2016, 33: 93-107.

[15] NianFeng W, ChaoYu C, Hao G, et al. Advances in dielectric elastomer actuation technology[J]. Science China(Technological Sciences), 2018, 61(10): 1512-152